ELSEVIER

www.elsevier.nl/locate/jorganchem

Journal of Organometallic Chemistry 609 (2000) 95–103

Journal of Organometallic Chemistry

H_2 binding to and silane alcoholysis on an electrophilic Mn(I) fragment with tied-back phosphite ligands. X-ray structure of a $Mn–CH_2Cl_2$ complex

Xinggao Fang, Jean Huhmann-Vincent, Brian L. Scott, Gregory J. Kubas *

Chemical Science and Technology Division, MS J514, Los Alamos National Laboratory, Los Alamos, NM 87545, USA

Received 20 January 2000; received in revised form 16 April 2000

Abstract

The solvent-coordinated cationic complex [*mer*-$Mn(CO)_3\{P(OCH_2)_3CMe\}_2(ClCH_2Cl)][BAr_F]$ (**4**), has been prepared by the reaction of the methyl precursor *mer*-$Mn(Me)(CO)_3\{P(OCH_2)_3CMe\}_2$ with $[Ph_3C][BAr_F]$. The coordinated solvent, CH_2Cl_2, binds to Mn through one chloride atom in the X-ray crystal structure, which also exhibits novel interligand hydrogen bonding between an acidic hydrogen on CH_2Cl_2 and an oxygen of the phosphite. **4** binds H_2 in equilibrium fashion, and the η^2-H_2 complex has a very high J_{HD} of 34.5 Hz indicative of the high electrophilicity of the metal center. Silanes also displace the bound CH_2Cl_2 at low temperature, although the η^2-Si–H bond undergoes heterolytic cleavage on warming. **4** catalyzes reaction of $SiHEt_3$ with phenol to give Et_3SiOPh and H_2. The bound CH_2Cl_2 in **4** is displaced irreversibly by olefins, ethers, and amines, to form stable adducts. The cationic $[Mn(CO)_3(P(OCH_2)_3CMe)_2]^+$ fragment is more electrophilic than phosphine analogues, and the tied-back phosphites give less steric congestion and, importantly, cannot engage in agostic interactions that would compete with external ligand binding. The results in these and other related systems bring to the forefront the subtle balance between electronic and steric forces that occur on addition of sixth ligands to 16 e^- metal fragments.

Keywords: Manganese; Dichloromethane; Dihydrogen; Silane; Phosphite; Cyclooctene

1. Introduction

The coordination and activation of small molecules such as H_2 and silanes by formally 16 e^- electrophilic transition metal complexes has drawn considerable recent attention [1–5]. The binding properties of H_2 σ ligands are dependent primarily upon the electronic environment of the metal complexes, but steric factors can be critical for larger σ ligands such as silanes (SiH_nR_{4-n}; $n = 1–3$), olefins, and alkanes. Generally, cationic electrophilic metal centers with CO ligands favor formation of σ complexes of H_2 and silanes over oxidative addition to hydrides and silyl(hydrides) because the weak M → L backdonation cannot promote X–H bond cleavage. In particular, electrophilic manganese complexes, $[Mn(CO)(dppe)_2]^+$ (**1**) [6,7], and $[Mn(CO)_3(PCy_3)_2]^+$ (**2**) [8], and its Re analogue [9], all of which contain agostic C–H interactions (Scheme 1), were recently reported to reversibly weakly bind H_2 in place of the C–H.

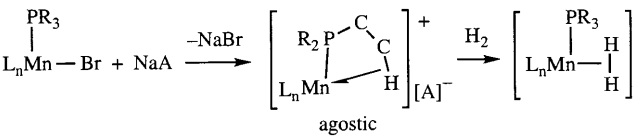

(1)

Such cationic agostic complexes, which of necessity contain low-coordinating BAr_F^- ($B[C_6H_3(3,5\text{-}CF_3)_2]_4^-$) anions, can be prepared according to Eq. (1) by metathesis of a metal halide with $NaBAr_F$ [6–8]. They can possess multiple internal C–H interactions as in **1**, and are valuable synthetic precursors for coordination of relatively weak ligands such as H_2. However, other weak ligands, including both π-acceptors such as SiH_3Ph, and σ bases such as Et_2O or CH_2Cl_2 do not coordinate (silane reactions with the Re species were not reported [9]). Presumably organosilane binding does not occur for steric reasons because SiH_3Ph does

* Corresponding author. Fax: +1-505-6673314.
E-mail address: kubas@lanl.gov (G.J. Kubas).

0022-328X/00/$ - see front matter
PII: S0022-328X(00)00230-8

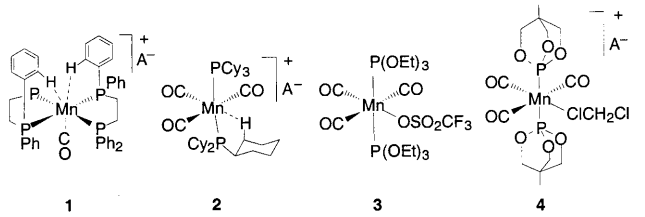

Scheme 1.

bind to isoelectronic, neutral $W(CO)_3(PCy_3)_2$ and is activated towards oxidative addition [10]. Third row metals such as W have a larger coordination sphere and less steric congestion than first row metal such as Mn.

Possibly because of steric effects, weak bases such as Et_2O and CH_2Cl_2 do not displace the agostic interaction in $M(CO)_3(PCy_3)_2$ ($M = W$, Mn^+, Re^+), but they do form isolatable adducts with a more electrophilic 16 e^- fragment with four electron-withdrawing CO ligands and only one phosphine, $[Re(CO)_4(PR_3)]^+$ ($R =$ Cy, *i*-Pr, Ph). The latter has been isolated only as six coordinate solvento species, $[Re(CO)_4(PR_3)(S)]^+$ ($S =$ Et_2O, CH_2Cl_2, pentafluoropyridine) [11,12], and an agostic precursor complex has not been observed, although the weakly-bound CH_2Cl_2 is displaceable by H_2 Eq. (2) [11,13].

$$L_nRe-CH_3 + HA \xrightarrow[-CH_4]{S} [L_nRe-S]A \xrightarrow{H_2} [L_nRe-H_2]A + S \quad (2)$$

The above Re solvento [11,12] or agostic [9] complexes were prepared by treatment of the methyl complexes with acids (Eq. (2)), or alternately for the former, with $[Ph_3C][BAr_F]$ to give Ph_3CMe and $[Re(CO)_4(PCy_3)(S)]^+$.

Another synthetic option for preparing such precursors or H_2 complexes is protonation of a hydride to directly give the H_2 complex or a precursor complex via rapid H_2 elimination, if the H_2 complex is very labile. For example, the protonation of the phosphite complex, *mer*-$MnH(CO)_3P_2$ ($P = P(OEt)_3$), with CF_3SO_3H at low temperature afforded in this case a neutral anion-coordinated complex, $Mn(CO)_3P_2(\eta^1\text{-}OSO_2CF_3)$ (**3**) (Scheme 1), without detection of the cationic H_2 complex formed initially [14].

$$MnH(CO)_3P_2CF_3SO_3H \xrightarrow{Et_2O} [Mn(CO)_3P_2(H_2)]$$
$$CF_3SO_3^- \xrightarrow{-H_2} Mn(CO)_3P_2(\eta^1\text{-}OSO_2CF_3) \quad (3)$$

The failure in detecting H_2 complexation in Eq. (3) is presumably due to the immediate coordination of $CF_3SO_3^-$, which unlike BAr_F is not a low-coordinating anion. The same type of reaction carried out in ethanol using aqueous HBF_4 as the acid yielded the aquo complex $[Mn(CO)_3(P)(H_2O)]BF_4$ ($P = PPh(OEt)_2$), which can be considered a 'solvento-type' complex, where the water from the acid binds to the metal center instead of the anion. Similarly, protonation of *mer*-$MnH(CO)_3(PP)$ ($PP =$ dppe or depe) with $HBF_4 \cdot Et_2O$ in $CHCl_3$ at r.t. afforded $[Mn(CO)_3(PP)(H_2O)]BF_4$ [15], where the water is from adventitious sources (H_2O is clearly a stronger ligand here than BF_4, a known coordinating anion). Thus there are four different synthetic routes to four possible reaction products in these systems: (a) a solvento complex, (b) an anion-coordinated species, (c) an agostic complex or (d) an H_2 complex. The trends for (a)–(d) formation cannot be predicted and depend on several factors including the electrophilicity of the metal center, sterics and relative binding strengths of the sixth ligand. Entropy effects play a large role here, and agostic binding can be favored by up to 10 kcal mol^{-1} over external ligand coordination

It would be of interest to further tune the steric and electronic properties of analogous Mn(I) complexes with phosphorus donor ligands and low-coordinating anions. The tied-back phosphite ligand, $P(OCH_2)_3CMe$ in **4** is of interest here for several reasons. It is both a weaker σ-donor and a stronger π-acceptor than analogous phosphines, and should increase the electrophilicity of the metal center. Most importantly, unlike **2**, it lacks accessible C–H bonds to form agostic interactions that would compete with binding of very weak external ligands, e.g. alkanes.

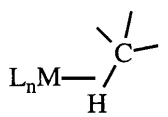

σ alkane complex

Such σ complexes are being highly sought for studies of C–H activation, but ΔH of binding is at best only 10–15 kcal mol^{-1}, which is not enough to overcome the entropic advantage for internal agostic C–H coordination. A stable (or even transient) 16 e^- fragment that cannot possess competing agostic interactions is necessary for observing σ-alkane coordination, which is an intermediate in alkane activation on for example highly electrophilic cationic platinum complexes [16–18]. Also, $CpRe(CO)_2$(cyclopentane) has been observed by NMR at low temperature [19], so Group 7 carbonyl complexes are appropriate targets for isolation of alkane complexes.

The tied-back phosphite is also sterically more compact than phosphines and may accommodate alkanes, silanes, olefins, and other more sterically demanding ligands in first-row metals. Here we would like to report the synthesis of **4** and other adducts of a highly electrophilic cationic 16 e^- Mn(I) fragment with tied-back phosphite ligands and a weakly coordinating BAr_F

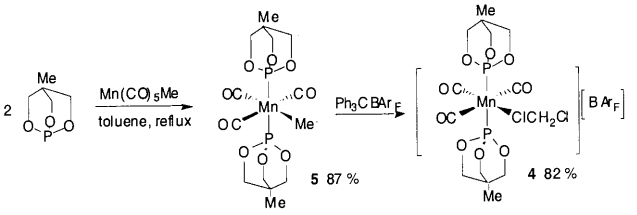

Scheme 2.

Table 1
Crystal data and structure refinement for complex **4**

Empirical formula	$C_{46}H_{32}BCl_2F_{24}MnO_9P_2$
Crystal size (mm^3)	$0.04 \times 0.08 \times 0.25$
Temperature (K)	203(2)
Wavelength (Å)	0.71073
Space group	Triclinic, $P\bar{1}$
Unit cell dimensions	
a (Å)	13.0850(7)
b (Å)	14.5411(7)
c (Å)	15.0947(8)
α (°)	93.482(1)
β (°)	104.105(1)
γ (°)	98.799(1)
Z	2
Theta range for data collection (°)	1.4–26.4
Reflections collected	14 134
Independent reflections	10 116 [$R_{int} = 0.0196$]
Final R indices [$I > 2\sigma(I)$]	$R_1 = 0.0716$, $wR_2 = 0.2035$
R indices (all data)	$R_1 = 0.0964$, $wR_2 = 0.2217$

anion. The labile dichloromethane ligand in the valuable synthon **4** can be displaced by H_2, ethers, amines, olefins and silanes, which undergo heterolytic cleavage. Facile heterolytic cleavage of both H_2 and silanes are observed on the cationic system $[Re(CO)_4(PR_3)(L)]^+$ [11,13].

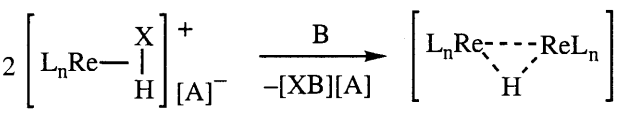

(4)

Bound H_2 can be highly acidic on cationic systems (pK_a near zero or less) and can readily protonate ethers or other weak bases B as in Eq. (4) [1]. Cationic silane σ complexes can be observed at low temperature but are nearly always unstable towards heterolytic cleavage at room temperature (r.t.) [13,20]. The Mn–phosphite system offers an opportunity for further study of these types of reactions, which in principle may occur for alkane activation.

2. Results and discussion

2.1. Dichloromethane complex (4)

The cationic dichloromethane complex **4** is prepared in high yield as outlined in Scheme 2. Treatment of $Mn(CO)_5Me$ [21] with two equivalents of $P(OCH_2)_3CMe$ (1-methyl-4-phospha-3,5,8-trioxabicyclo[2.2.2]octane) [22] in refluxing toluene yields the tricarbonyl methyl complex **5**. The *mer*-configuration of **5** is shown by the IR CO stretching (ν_{CO}) pattern: 2035 w, 1952 s, 1926 s. Reaction of **5** with $[Ph_3C][BAr_F]$ [23] in CH_2Cl_2 leads to the CH_2Cl_2 complex **4** as yellow crystals in 82% yield. The ν_{CO} values for **4** (in CD_2Cl_2), 2096 w, 2025 s and 2004 s, are much higher than those (2048 w, 1962 s, and 1942 s) of the phosphine analogue **2** (where an agostic interaction takes the place of CH_2Cl_2). This is a result of weaker backdonation from Mn to the CO ligands in **4** and suggests that the Mn(I) center in **4** is significantly more electrophilic than that in **2**. The ^{1}H-NMR spectrum of **4** shows a resonance at 5.33 ppm corresponding to the free CH_2Cl_2 (free exchange with the solvent, CD_2Cl_2, occurs). In contrast, the less electrophilic and more sterically demanding **2** does not bind CH_2Cl_2 [8]. The bound CH_2Cl_2 cannot be removed from solid **4** by exposure to high vacuum for hours, but can be displaced in solution by H_2 and other ligands as will be shown below. As for **1** and **2**, N_2 does not react with **4**, presumably because N_2 is a very poor σ donor, weaker even than CH_2Cl_2. In contrast to **4**, the analogue **3** with non tied-back phosphites is found to coordinate the $CF_3SO_3^-$ anion instead of CH_2Cl_2 solvent [14]. This demonstrates the importance of using the low-coordinating BAr_F anion because anions such as $CF_3SO_3^-$ are stronger ligands than CH_2Cl_2 and perhaps other small molecules of interest here, e.g. H_2. Also in this regard, all mononuclear dichloromethane complexes are cationic because CH_2Cl_2 is a very poor base and coordinates only to strong metallo Lewis acids.

Only a handful of dichloromethane complexes have been structurally characterized, and coordination can be monodentate [11,12,24], bidentate as in the first CH_2Cl_2 complex characterized by X-ray diffraction by Strauss and coworkers [25,26], or bridging via both Cl in a Ru_3 cluster [27]. In order to determine the geometry in **4**, single crystals were grown from mixed CH_2Cl_2 and hexane solvents and were subjected to X-ray structural analysis (Table 1 and Fig. 1). The complex shows typical octahedral configuration with *trans*-phosphite ligands. The CH_2Cl_2 molecule is bound to Mn through one chlorine atom Cl(1) with a Mn–Cl(1) distance of 2.4109(13) Å. The average Mn–P distance, 2.2281(12) Å, is shorter than that found in **2**, 2.354 Å. Regarding the metal–CO bonding, the distance for Mn–C(2) *trans* to the bound CH_2Cl_2, 1.803(3) Å, is much shorter than

the Mn–C(1) and Mn–C(3) distances of 1.867(5) and 1.880(5) Å, respectively. This reflects a strong *trans* effect: the nearly pure base CH_2Cl_2 does not compete for backdonation with the CO *trans* to it unlike the situation for the other two CO ligands that are *trans* to one another. Hence the Mn–C(2) bond is stronger than the other M–CO bonds, and M–C distances generally decrease as the π-acceptor strength of the ligand *trans* to CO decreases. Several closely-related Group 6 and 7 complexes show this behavior [7], especially **2** where the weak agostic interaction (with virtually no π-acceptor strength) is *trans* to the CO and the Mn–C distance is even shorter, 1.761(7) Å [8]. The C(4)–Cl(1) distance for the bound Cl, 1.804(5) Å, is longer than the 1.720(7) Å distance for the terminal C(4)–Cl(2), as has been observed in similar octahedral Re(I) complexes, $[Re(CO)_4(PR_3)(CH_2Cl_2)]^+$ [11,12] and other monodentate CH_2Cl_2 complexes [24]. The C(1)–Mn(1)–C(3) angle 179.0(2)° is very close to linear while that for C(2)–Mn(1)–Cl(1), 173.96(16)°, shows the two bonds C(2)–Mn(1) and Cl(1)–Mn(1) to be slightly bent away from linearity.

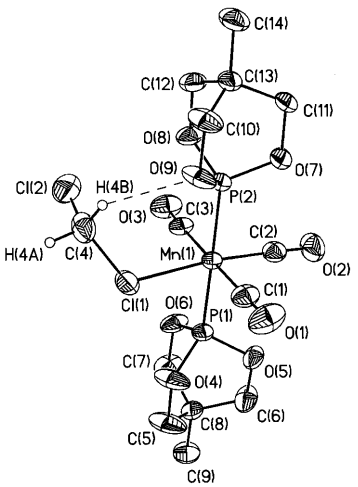

Fig. 1. Ortep diagram for complex **4**. Selected bond distance (Å) and bond angles (°): Mn–C(1) = 1.867(5), Mn–C(2) = 1.803(3), Mn–C(3) = 1.880(5), Mn–P(1) = 2.2328(12), Mn–P(2) = 2.2234(12), Mn–Cl(1) = 2.4109(13), Cl(1)–C(4) = 1.804(5), Cl(2)–C(4) = 1.720(7), C(4)–O(9) = 3.185(6), H(4B)–O(9) = 2.418 (idealized H), C(1)–Mn–C(3) = 179.0(2), C(2)–Mn–Cl(1) = 173.69(16), P(1)–Mn–P(2) = 176.97(5), C(3)–Mn–Cl(1) = 93.59(15), C(1)–Mn–Cl(1) = 86.52(16), P(1)–Mn–Cl(1) = 86.47(4), P(2)–Mn–Cl(1) = 94.53(5), Cl(1)–C(4)–Cl(2) = 112.1(3), Mn–Cl(1)–C(4) = 118.2(2).

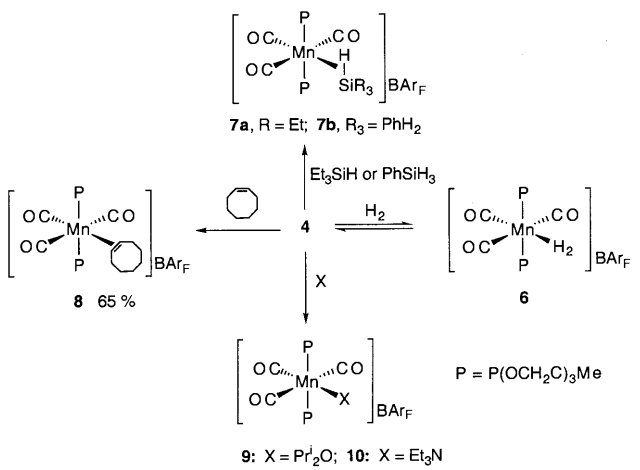

Scheme 3.

A weak interligand hydrogen bonding interaction appears to occur in **4** between an acidic hydrogen on CH_2Cl_2 and an oxygen atom on the phosphite ligand. The distance between O(9) and an idealized hydrogen position H(4B) is calculated to be 2.418 Å, well within the general range for C–H···O hydrogen bonds [28,29], which for example can involve the oxygen of CO ligands in metal complexes [30]. The distance between C(4) and O(9), 3.185(6) Å, is within the short end of the range (3.0–4.0 Å) for such an interaction, although the C–H···O angle, 135.7°, is more acute than normal. Hydrogen bonding involving haloalkanes is common, and the hydrogens on the CH_2Cl_2 ligand might be expected to be more acidic than in free dichloromethane because the electrophilic metal is withdrawing electrons from Cl. The coordination geometry of the CH_2Cl_2 ligand is not distorted from that in related complexes. A precedent for any type of hydrogen bonding to an oxygen atom of a phosphite ligand was not located in a literature search. The hydrogen bonding interaction energy in **4** can be estimated to be several kcal mol^{-1}, which may help stabilize the CH_2Cl_2 coordination.

2.2. Dihydrogen complex (6)

Exposure of a yellow solution of **4** in CD_2Cl_2 to ca. 3 atm of H_2 gave a similarly colored solution that showed a broad signal at −9.19 ppm in the temperature range of −60 to 25°C. The peak is attributed to the σ-bound H_2 ligand in **6** that is presumably undergoing equilibrium exchange with CH_2Cl_2–CD_2Cl_2 (Scheme 3). Integration showed that only about 2–3% H_2 complex was present, but this merely reflects the much greater concentration of CD_2Cl_2 over H_2 rather than relative ligand binding strengths (H_2 may actually be the stronger ligand). The ^{31}P-NMR chemical shifts for **6** and **4** are virtually identical, δ 155.1 and 155.2, respectively, indicating similar net ligand effects for H_2 and CH_2Cl_2 (although these ligands are not electronically similar because H_2 is a moderate π-acceptor). Replacement of H_2 with HD gas afforded the η^2-HD complex, [*mer*-$Mn(CO)_3\{P(OCH_2)_3CMe\}_2(HD)][BAr_F]$, which showed a J_{HD} coupling of 34.5 Hz (J_{PH} is not seen because the peaks are too broad, as for most HD or H_2 complexes). As can be seen in Table 2, this is the highest value found for any Mn–Re phosphite–phos-

Table 2
J_{HD} coupling constants and H–H distances for H_2 complexes of Group 7 fragments with *trans*-CO ligands

Metal fragment	J_{HD} (Hz)	H–H (Å) [a]	Reference
$[Mn(CO)(dppe)_2]^+$ (**1**)	32	0.89–0.90	[6]
$[Mn(CO)(depe)_2]^+$	33	0.87–0.89	[7]
$[Mn(CO)\{P(OEt)_3\}_4]^+$	32	0.89–0.90	[14]
$[Mn(CO)\{PPh(OEt)_2\}_4]^+$	32.5	0.88–0.89	[14]
$[Mn(CO)_2\{P(OEt)_3\}_3]^+$	33	0.87–0.89	[14]
$[Mn(CO)_3(L)_2]^+$ [b] (**6**)	34.5	0.84–0.86	This work
$[Mn(CO)_3(PCy_3)_2]^+$ (**2**)	33	0.87–0.89	[8]
$[Re(CO)_4(PCy_3)]^+$	33.8	0.85–0.87	[11]
$[Re(CO)_3(PCy_3)_2]^+$	32	0.89–0.90	[9]
$[Re(CO)_3(PPr^i_3)_2]^+$	33	0.87–0.89	[9]
$[Re(CO)_3\{P(OEt)_3\}_2]^+$	30	0.92–0.94	[37]
$[Re(CO)_2(PMe_2Ph)_3]^+$ [c]	31	0.90–0.92	[20]
$[Re(CO)_2\{P(OEt)_3\}_3]^+$	33	0.87–0.89	[37]
$[Re(CO)\{P(OEt)_3\}_4]^+$ [c]	33	0.87–0.89	[37]

[a] Except where noted, calculated from and bracketed by the empirical relationships, $r_{HH} = 1.42 - 0.0167$; J_{HD} [32] and $r_{HH} = 1.44 - 0.0168$; J_{HD} [33].
[b] $L = P(OCH_2)_3CMe$.
[c] In equilibrium with dihydride tautomer in solution.

phine complex with varying numbers of CO ligands and is among the highest ever reported (35 Hz for $Cr(CO)_3(P^iPr_3)_2(HD)$ is the highest; H–H = 0.85 Å [31]). This is consistent with η^2-H_2 binding to a highly electrophilic metal center with a relatively short H–H distance (calculated [32,33] to be 0.84–0.86 Å from J_{HD}). In all cases CO is *trans* to H_2 in Table 2, and the nature of the *trans* ligand exerts by far the greatest influence on properties such as J_{HD} and H–H distance [7]. However, the *cis* ligands do have some effect, although not always according to the expected trends, e.g. J_{HD} might have been expected to be reversed for the dppe versus the more electron-rich depe Mn complex (which should elongate the H–H bond more). Also the trends for Re phosphite and phosphine complexes are the reverse of what might have been expected electronically, e.g. $[Re(CO)_3\{P(OEt)_3\}_2]^+$ has a lower J_{HD} than that for $[Re(CO)_3(PCy_3)_2]^+$. Thus the very high J_{HD} for **6** might be somewhat anomalous, although it is not contrary to expected trends.

Regarding the lability of the H_2 ligand in **6** in solution, the bound H_2 is readily displaced by CH_2Cl_2 when the H_2 atmosphere is released by exposure of the solution to a He atmosphere. This is similar to the behavior for $Cr(CO)_3(P^iPr_3)_2(H_2)$ and other highly labile H_2 complexes, and it appears that the H_2 in **6** is more weakly bound than the H_2 coordinated to the less electrophilic Mn fragments **1** and **2**. For example, 95% of complex **2** was found to be bound to H_2 at −10°C under similar conditions. A possible explanation is that the bulky phosphine groups in $[Mn(CO)_3(PCy_3)_2(H_2)]^+$ inhibit displacement of the H_2 by the solvent, CH_2Cl_2.

The H_2 ligand in **6** does not appear to be as prone towards heterolytic cleavage as that in $[Re(CO)_4(PR_3)(H_2)]^+$ (Eq. (4)), where protonation of ethers such as $^iPr_2O$ readily occurs [11]. An analogous experiment was performed in which H_2 was added to a solution of **4** in CD_2Cl_2 at liquid nitrogen temperature to form **6**, which was then warmed to −78° and treated with ca. 1.5 μl of $^iPr_2O$ (ca. three equivalents). ^{1}H- and ^{31}P-NMR spectra were recorded from −80 to 25°, but only the $^iPr_2O$ complex **9** (see below) and free H_2 were observed at all temperatures. Similarly, reaction of **4** with $^iPr_2O$ followed by addition of H_2 (3 atm) at −198°C and warming gave only **9**. Although the stronger binding of the ether than H_2 may interfere with a potential H_2 heterolytic cleavage process, the acidity of the bound H_2 is probably lower than that in $[Re(CO)_4(PR_3)(H_2)]^+$. In the latter, formation of a hydride-bridged dinuclear species on deprotonation as in Eq. (4) is thermodynamically very favorable, but such a complex (or a mononuclear hydride) is not seen for the Mn system here.

2.3. Binding, heterolytic cleavage, and alcoholysis of silanes

When a CD_2Cl_2 solution of **4** was treated with 1.2 equivalents of Et_3SiH at −78°C, a yellow solution was generated which showed a triplet at high field, $\delta = -16.1$ ($J_{HP} = 15.9$ Hz), corresponding to one proton. When $PhSiH_3$ was used in place of Et_3SiH, a similar ^{1}H-NMR signal appeared at δ −15.3 ($J_{HP} = 15.5$ Hz) corresponding to ca. 0.2 proton, i.e. about 20% complexation by the silane (recorded at −60°C; no reaction occurs at −80°C here). In addition, the ^{31}P-NMR spectra showed a new signal at 159.3 ppm along with the 155.6 ppm peak from the starting **4**. These new signals presumably represent an η^2-bound R_3Si–H complex **7** similar to structurally-characterized $Mo(CO)(\eta^2$-H–$SiR_3)(diphosphine)_2$ [34] and $[Re(CO)_4(PR_3)(\eta^2$-H–$SiEt_3)]^+$ observed by low-temperature NMR [13]. As in the latter, the J_{HP} coupling constants are too small for a Mn–H complex (typical $J_{HP} = 40$–60 Hz [14,35]). J_{SiH} could not be measured due to the Mn quadruplar broadening. When the mixtures were raised to r.t., the high field proton signal disappeared, and the ^{1}H-NMR spectra indicated the formation of a mixture of several unidentified products that were likely formed by heterolytic cleavage of the η^2-Si–H bond as for the Re complex [13]. No clear evidence was present for formation of a Mn hydride complex, either as an intermediate or a final product. GC–MS analysis of the volatiles released from **7a** showed $(Et_3Si)_2O$ to be the major component, which is presumably generated from reaction of the silyl cation with adventitious moisture as for $[Re(CO)_4(PR_3)(HSiEt_3)]^+$ as well as a $[CpFe(CO)(PPh_3)(HSiR_3)]^+$ system [36].

$$2[Mn(Et_3SiH)]^+ \rightarrow 2Et_3Si^+ \xrightarrow{H_2O} (Et_3Si)_2O + 2H^+ \quad (5)$$

As mentioned in Section 1, this is typical behavior for a cationic silane complex because the Si atom of the Si–H bond is highly activated toward nucleophilic attack on account of depletion of the electron density of the Si–H bond on coordination to cationic metal centers.

The fate of the Mn fragment is not shown in Eq. (5) but it is conceivable that if a Mn–H species forms it could be immediately protonated to the H_2 complex **6** by the protons released from silane hydrolysis in Eq. (5). The labile H_2 in **6** could then be displaced by CH_2Cl_2 solvent, to regenerate **4** in the absence of excess H_2.

$$[Mn(Et_3SiH)]^+ \underset{\mathbf{7a}}{} \rightarrow [Mn(H)] \underset{\text{unobserved}}{} \xrightarrow{H^+} [Mn(H_2)]^+ \underset{\mathbf{6}}{}$$
$$\xrightarrow[-H_2]{CH_2Cl_2} [Mn(CH_2Cl_2)]^+ \underset{\mathbf{4}}{} \quad (6)$$

Such formation of $[CpFe(CO)(PPh_3)(H_2)]^+$ from hydrolysis of $[CpFe(CO)(PPh_3)(HSiR_3)]^+$ has previously been observed and employed for catalytic silane alcoholysis [36]. The Mn system also catalyzes reaction of phenol with triethylsilane, presumably by a mechanism similar to that proposed for the Fe system (Scheme 4). The ratio of silane (0.307 mmol) to the precatalyst **4** was about 24:1, and a slight deficiency of phenol (0.287 mmol) was added at −78°C in a NMR tube reaction. ^{1}H-NMR spectra recorded from −80°C to 25°C all showed a broad signal at −9.23 ppm presumably due to the H_2 complex formed according to Scheme 4. Upon exposure of the solution in the NMR tube to a He atmosphere after reaction was complete, the ^{1}H-NMR spectrum showed a triplet at −16.75 ppm corresponding to the silane σ complex, **7a**. The latter would be expected according to Scheme 4 since unreacted silane was present (stoichiometric excess over phenol reactant) and is a stronger ligand than either H_2 or CH_2Cl_2. The expected product of silane alcoholysis, $PhOSiEt_3$, was isolated in ca. 50% yield, demonstrating that the reaction is catalytic. Manganese carbonyl species such as $Mn(CO)_5(CH_3)$ and $[Mn(CO)_4Br]_2$ are also effective precatalysts for alcoholysis of silanes [38] and may operate via a similar pathway, i.e. the true catalyst is an electrophilic unsaturated Mn fragment that heterolytically cleaves an intermediate silane σ complex.

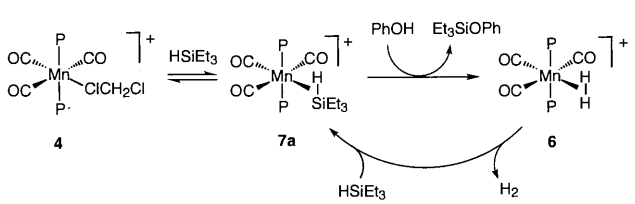

Scheme 4.

2.4. Olefin, ether, and amine complexes (8–10) and summary

Reaction of **4** with *cis*-cyclooctene (cco) afforded **8** as a yellow solid in 65% yield. The olefinic protons show a ^{1}H-NMR signal at 4.81 ppm, upfield shifted from the 5.67 ppm found for free cco. The cco cannot be removed under prolonged vacuum. Lastly, addition of ^{i}Pr$_2$O or Et_3N to CD_2Cl_2 solutions of **4** resulted in the respective ether or amine complexes **9** and **10**. All of these molecules appear tightly bound to the metal Mn, and none were in equilibrium with CD_2Cl_2 or H_2 under three atmospheres of hydrogen gas. The formation of the ^{i}Pr$_2$O complex is somewhat surprising since ^{i}Pr$_2$O does not bind to the $[Re(CO)_4(PPh_3)]^+$ fragment, although the latter does coordinate Et_2O [11,12]. That could mean the bis(phosphite) Mn complex is either more electrophilic than the Re monophosphine species, or has more room for coordination (or both electronic and steric factors are more favorable). There may be more steric interference of the ^{i}Pr groups with the phenyl groups on the single *cis* phosphine on Re than with the two tied-back phosphites on Mn.

In summary, the highly electrophilic $[Mn(CO)_3(P(OCH_2)_3CMe)_2]^+$ fragment with *trans* tied-back phosphite ligands binds dichloromethane solvent to form the structurally characterized complex **4**, isolated as a BAr_F salt. The latter contains novel interligand hydrogen bonding between an acidic hydrogen on the CH_2Cl_2 ligand and an oxygen of the phosphite. The coordination of CH_2Cl_2 is in direct contrast to the lack of binding by the phosphine analogues $[M(CO)_3(PCy_3)_2]^+$ (M = Mn, Re) that contain agostic interactions. Presumably the tied-back phosphites give less steric congestion and more electrophilic metal centers, and of course cannot engage in agostic interactions that would compete with external ligand binding. Under a hydrogen atmosphere, **4** is in equilibrium with the η^2-H_2 complex (**6**), and the very high J_{HD} for **6** points to the high electrophilicity of the metal center. Silanes also displace the bound CH_2Cl_2 at low temperature, but the η^2-Si–H bond undergoes heterolytic cleavage on warming. **4** catalyzes reaction of $SiHEt_3$ with phenol to give Et_3SiOPh and H_2. The CH_2Cl_2 ligand in **4** is irreversibly displaced by olefins, ethers and amines to form stable adducts. The results in these and other related systems bring to the forefront the subtle balance between electronic and steric forces that occur on addition of sixth ligands to 16 e^- metal fragments.

3. Experimental

All manipulations were performed either under a helium atmosphere in a Vacuum Atmospheres drybox or under an argon atmosphere using standard Schlenk

techniques unless otherwise specified. CH_2Cl_2 was distilled under Ar from P_2O_5. Toluene and hexane were purified by passing through an alumina column. Hydrogen gas was obtained from an in-house gas plant and was of UHP grade. HD gas was purchased from Isotec Inc. Other reagents were purchased from Aldrich, Acros or Strem Chemical Co. and used as received. ^{1}H-, ^{31}P-, ^{13}C- and ^{11}B-NMR spectra were recorded on a Varian Unity 300 spectrometer with field strengths of 300, 121, 75 and 96 MHz, respectively. ^{1}H and ^{13}C chemical shifts were referenced to the residual solvent resonance relative to TMS; ^{31}P and ^{11}B chemical shifts were referenced to external 85% H_3PO_4 and BF_3–Et_2O, respectively. Infrared spectra were recorded on a Nicolet Avator 360 FTIR spectrometer. Elemental analyses were performed in house on a Perkin–Elmer Series II CHNS/O model 2400 analyzer.

3.1. Preparation of *mer*-$Mn(P(OCH_2)_3CMe)_2(CO)_3(Me)$ (**5**)

A mixture of $Mn(CO)_5Me$ (0.210 g, 1.00 mmol) and $P(OCH_2)_3CMe$ (0.311 g, 2.10 mmol) in toluene (ca. 10 ml) was refluxed for ca. 16 h under Ar atmosphere to give a yellowish suspension. The mixture was then filtered and the solid washed with toluene (2 ×) and hexane (2 ×) to give an off-white solid. The solid was purified in air by flash silica-gel column chromatography eluting with CH_2Cl_2 to give the product (0.390 g, 87%) as a white solid. Anal. Calc. for $C_{14}H_{21}O_9P_2Mn$: C, 37.35; H, 4.70. Found: C, 37.16; H, 4.77%. FTIR (CD_2Cl_2, cm^{-1}) 2035 w, 1952 vs. 1926 s. ^{1}H-NMR (CD_2Cl_2), δ 4.20 (t, $J_{HP} = 2.2$ Hz, 12H, $P(OCH_2)_3CMe$), 0.76 (s, 6H, $P(OCH_2)_3CCH_3$), −0.62 (t, $J_{HP} = 8.0$ Hz, 3H, $MnCH_3$). ^{31}P-NMR (CD_2Cl_2), δ 167.7.

3.2. Preparation of [*mer*-$Mn(P(OCH_2)_3CMe)_2(CO)_3(ClCH_2Cl)][BAr_F]$ (**4**)

A yellow solution of **5** (0.101 g, 0.224 mmol) and $[Ph_3C][BAr_F]$ (0.248 g, 0.224 mmol) in CH_2Cl_2 (5 ml) was stirred at r.t. for 20 min. Hexane (15 ml) was then layered on top of the CH_2Cl_2 solution and the mixture was cooled at −30°C to give the product (0.238 g, 82%) as yellow crystals. Anal. Calc. for $C_{46}H_{32}BCl_2F_{24}O_9P_2Mn$: C, 39.91; H, 2.31. Found: C, 40.06; H, 2.52%. FTIR (CD_2Cl_2, cm^{-1}) 2096 w, 2025 vs. 2004 s. ^{1}H-NMR (CD_2Cl_2) δ 7.74 (s, 8H, BAr_F), 7.58 (s, 4H, BAr_F), 4.39 (t, $J_{HP} = 2.2$ Hz, 12H, $P(OCH_2)_3CCH_3$), 0.86 (s, 6H, $P(OCH_2)_3CCH_3$). ^{13}C-NMR (CD_2Cl_2), δ 15.1, 34.1, 77.6. ^{11}B-NMR (CD_2Cl_2), δ −12.1. ^{31}P-NMR (CD_2Cl_2), δ 155.2.

3.3. Reaction of **4** with H_2 to give **6**

A J-Young NMR tube was charged with **4** (0.020 g) and CD_2Cl_2. On a vacuum line, the yellow solution was frozen and evacuated, then backfilled at liquid N_2 temperature with H_2 (ca. 3 atm). The tube was closed off and warmed to r.t. to give a yellow solution. ^{1}H-NMR (CD_2Cl_2), δ −9.19 (br, s), 0.88 (s, 6H), 4.40 (t, 12H, J = 2.2 Hz), 7.56 (s, 4H), 7.72 (t, 8H, $J = 2.4$ Hz). ^{31}P-NMR (CD_2Cl_2), δ 155.1. The NMR spectrum obtained at −60°C was identical. However the complex partially decomposed while left standing at r.t. for ca. 16 h.

3.4. Reaction of **4** with silanes to give **7** and heterolytic cleavage

Et_3SiH (7.3 μl, 0.046 mmol) was injected into a 5 mm NMR tube containing **4** (49.4 mg, 0.038 mmol) in CD_2Cl_2 (0.5 ml) at −78°C to give a yellow solution. NMR spectra were recorded at −60°C. ^{1}H-NMR (CD_2Cl_2), δ −16.81 (t, $J_{HP} = 15.9$ Hz, Et_3Si–*H*), 0.87 (s, 6H), 1.06 (m, 15H), 4.37 (s, 12H), 7.62 (s, 4H), 7.78 (s, 12H). ^{31}P-NMR (CD_2Cl_2), δ 161.2. The NMR spectra recorded at progressively elevated temperatures of −40°C, −20°C and 0°C showed no apparent change. However at r.t. the complex decomposed to several unidentified products within 10 min.

On analogy, reaction of **4** with $PhSiH_3$ at −60°C gave a similar silane complex which decomposed at r.t. Relevant NMR data: ^{1}H-NMR δ −15.3 (t, $J = 15.3$ Hz, ca. 0.2 H). ^{31}P-NMR, δ 159.3, 155.6 (major).

3.5. Reaction of **4** with Et_3SiH and phenol

Et_3SiH (49 μl, 0.307 mmol) was injected into a 5 mm NMR tube containing **4** (17.0 mg, 0.013 mmol) at −78°C. Then a solution of phenol (27.0 mg, 0.287 mmol) in CD_2Cl_2 (ca. 0.6 ml) at ca. −40°C was transferred via cannula to give a yellow solution. ^{1}H-NMR spectra recorded from −80°C to 25°C all showed a broad signal at −9.23 ppm presumably due to the H_2 complex, **6**. ^{31}P-NMR (−80°C): δ 160.0 (major), 155.0 (minor); (−40°C) 160.3; (0°C) 160.5; (25°C) 161.0. After the solution in the NMR tube was exposed to a He atmosphere, NMR spectra were recorded immediately at RT. The ^{1}H-NMR spectrum showed a triplet at −16.75 ppm with a coupling constant of 15.5 Hz, and the ^{31}P-NMR showed a singlet at 161.4 ppm. These signals correspond to the silane σ complex (**7a**). $PhOSiEt_3$ was isolated in ca. 50% yield by chromatography on a silica gel column and identified by GC–MS and NMR data.

3.6. Preparation of [mer-$Mn(P(OCH_2)_3CMe)_2(CO)_3$-(cis-cyclooctene)][$BAr_F$] (**8**)

To a mixture of **5** (74.3 mg, 0.165 mmol) and [Ph_3C][BAr_F] (182.6 mg, 0.165 mmol) was added *cis*-cyclooctene (0.1 ml, 0.768 mmol) followed by CH_2Cl_2 (2 ml) at 25°C. The resulting yellow solution was stirred for 30 min. Hexane (12 ml) was layered on top of the CH_2Cl_2 solution, and the mixture was cooled to −30°C to give the product (0.151 g, 65%) as a light yellow solid. Anal. Calc. for $C_{53}H_{44}BF_{24}O_9P_2Mn\cdot 0.5CH_2Cl_2$: C, 44.26; H, 3.10. Found: C, 44.60; H, 3.33%. FTIR (CD_2Cl_2, cm^{-1}) 2083 w, 2013 vs. (br). ^{1}H-NMR (CD_2Cl_2), δ 0.79 (s, 6H), 1.53 (m, 6H), 1.85 (m, 2H), 2.05 (m, 2H), 2.35 (dd, 2H, $J = 13.4$, 3.4 Hz), 4.25 (t, 12H, $J = 2.2$ Hz), 4.81 (m, 2H, C*H*CH2), 7.57 (s, 4H), 7.73 (s, 12H). ^{13}C-NMR (CD_2Cl_2) δ 15.0, 26.2, 28.3, 31.5, 33.6 (*C*Me), 77.3 (OCH_2), 101.6 (*C*HCH_2). ^{31}P-NMR (CD_2Cl_2), δ 157.2.

3.7. Reaction of **4** with isopropyl ether and H_2 to give **9**

To a solution of **4** (20 mg) in CD_2Cl_2 (0.5 ml) in a J-Young NMR tube at 25°C was added $^iPr_2O$ (ca. 4 μl, 1.2 equivalent) to give a yellow solution. The mixture was then charged with H_2 under liquid N_2 temperature (ca. 3 atm), and NMR spectra were recorded at temperatures progressively from −60 to 25°C. Neither the H_2 complex **6** nor a hydride complex was observed within the chemical shift ranges of 20 to −30 ppm. H_2 was then released and NMR spectra were recorded at 25°C showing the presence of the ether complex **9**. FTIR (CD_2Cl_2, cm^{-1}) 2092 w, 2017 vs., 1982 s. ^{1}H-NMR (CD_2Cl_2), δ 0.88 (s, 6H), 1.10 (d, 12H, $J = 6.1$ Hz, ether OCHC*H*$_3$), 3.68 (hept, 2H, $J = 6.1$ Hz, ether OC*H*), 4.38 (t, 12H, $J = 2.2$ Hz), 7.57 (s, 4H), 7.73 (s, 8H). ^{13}C-NMR (CD_2Cl_2), δ 22.6, 22.8, 69.3 (ether OCH), 76.9 (OCH_2). ^{31}P-NMR (CD_2Cl_2), δ 156.5. Data for free $(Me_2CH)_2O$: ^{1}H: 3.63 ppm (OC*H*, same pattern and J as bound ether); ^{13}C: 68.0 (O*C*H).

3.8. Reaction of **4** with triethylamine and H_2 to give **10**

Same procedures were followed as for the reaction with isopropyl ether. FTIR (CD_2Cl_2, cm^{-1}), 2092w, 1999s, 1957s. ^{1}H-NMR (CD_2Cl_2), δ 0.82 (s, 6H), 0.98 (t, $J = 7.1$ Hz, NCH_2CH_3, free Et_3N), 1.34 (t, 9H, $J = 7.3$ Hz, coordinated NCH_2CH_3), 2.48 (quartet, $J = 7.1$ Hz, NCH_2, free Et_3N), 3.30 (quartet, 6H, $J = 7.3$ Hz, coordinated NCH_2), 4.30 (t, 12H, $J = 2.2$ Hz), 7.56 (s, 4H), 7.72 (s, 8H). ^{31}P-NMR (CD_2Cl_2), δ 156.2.

3.9. X-ray structure determination of **4**

A yellow, needle-shaped crystal of **4** was attached to a glass fiber using a spot of silicone grease. The air-sensitive crystal was mounted from a matrix of mineral oil under argon gas flow. The crystal was immediately placed on a Bruker P4/CCD/PC diffractometer, and cooled to 203 K using a Bruker LT-2 temperature device. The data were collected using a sealed, graphite monochromatized Mo–K_α X-ray source. A hemisphere of data was collected using a combination of φ and ω scans, with 20 s frame exposures and 0.3° frame widths. Data collection and initial indexing and cell refinement were handled using SMART software [39]. Frame integration and final cell parameter calculation were carried out using SAINT software [40]. The data were corrected for absorption using the SADABS program [41]. Decay of reflection intensity was not observed.

The structure was solved in space group $P\bar{1}$ using direct methods and difference Fourier techniques. The initial solution revealed the manganese, and the majority of all non-hydrogen atom positions. The remaining atomic positions were determined from subsequent Fourier synthesis. Hydrogen atom positions were fixed in ideal geometries (C–H = 0.93 for aromatic, 0.97 for methylene and 0.96 Å for methyl). The hydrogen atoms were refined using the riding model, with isotropic temperature factors fixed to 1.5 (methyl) or 1.2 (methylene and aromatic) times the equivalent isotropic U of the carbon atom they were bound to. The final refinement [42] included anisotropic temperature factors on all non-hydrogen atoms, and converged with final residuals of $R_1 = 0.0716$ and $R_{2w} = 0.2035$. Structure solution, refinement, graphics, and creation of publication materials were performed using SHELXTL NT [43].

4. Supplementary material

Crystallographic data for the structural analysis has been deposited with the Cambridge Crystallographic Data Centre, CCDC no. 139109 for compound **4**. Copies of this information may be obtained free of charge from The Director, CCDC, 12 Union Road, Cambridge, CB2 1EZ, UK (Fax: +44-1223-336033; e-mail: deposit@ccdc.cam.ac.uk or www: http://www.ccdc.cam.ac.uk).

Acknowledgements

This work was supported by the Department of Energy, Office of Basic Energy Sciences, Chemical Sciences Division. J.H.V. is grateful to the Director of the Los Alamos National Laboratory for postdoctoral funding.

References

[1] P.G. Jessop, R.H. Morris, Coord. Chem. Rev. 121 (1992) 289.
[2] D.M. Heinekey, J.W.J. Oldham, Chem. Rev. 93 (1993) 913.
[3] R.H. Crabtree, Angew. Chem. Int. Ed. Engl. 32 (1992) 789.
[4] J.Y. Corey, J. Braddock-Wilking, Chem. Rev. 99 (1999) 175.
[5] J.J. Schneider, Angew. Chem. Int. Ed. Engl. 35 (1996) 1068.
[6] W.A. King, X.L. Luo, B.L. Scott, G.J. Kubas, D.W. Zilm, J. Am. Chem. Soc. 118 (1996) 6782.
[7] W.A. King, B.L. Scott, J. Eckert, G.J. Kubas, Inorg. Chem. 38 (1999) 1069.
[8] A. Toupadakis, G.J. Kubas, W.A. King, B.L. Scott, J. Huhmann-Vincent, Organometallics 17 (1998) 5315.
[9] D.M. Heinekey, C.E. Radzewich, M.H. Voges, B.M. Schomber, J. Am. Chem. Soc. 119 (1997) 4172.
[10] M.D. Butts, G.J. Kubas, X.L. Luo, J.C. Bryan, Inorg. Chem. 36 (1997) 3341.
[11] J. Huhmann-Vincent, B.L. Scott, G.J. Kubas, J. Am. Chem. Soc. 120 (1998) 6808.
[12] J. Huhmann-Vincent, B.L. Scott, G.J. Kubas, Inorg. Chem. 38 (1999) 115.
[13] J. Huhmann-Vincent, B.L. Scott, G.J. Kubas, Inorg. Chim. Acta 294 (1999) 240.
[14] G. Albertin, S. Antoniutti, M. Bettiol, E. Bordignon, F. Busatto, Organometallics 16 (1997) 4959.
[15] T.M. Becker, J.A. Krause-Bauer, C.L. Homrighausen, M. Orchin, Polyhedron 18 (1999) 2563.
[16] M.W. Holtcamp, L.M. Henling, M.W. Day, J.A. Labinger, J.E. Bercaw, Inorg. Chim. Acta 270 (1998) 467.
[17] L. Johansson, O.B. Ryan, M. Tilset, J. Am. Chem. Soc. 121 (1999) 1974.
[18] R.A. Periana, D.J. Taube, S. Gamble, H. Taube, T. Satoh, H. Fujii, Science 280 (1998) 560.
[19] S. Geftakis, G.E. Ball, J. Am. Chem. Soc. 120 (1998) 9953.
[20] X.L. Luo, R.H. Crabtree, J. Am. Chem. Soc. 111 (1989) 2527.
[21] R.D. Closson, J. Kozikowski, T.H. Coffield, J. Org. Chem. 22 (1957) 598.
[22] J.G. Verkade, T.J. Huttemann, M.K. Fung, Inorg. Chem. 4 (1965) 228.
[23] S.R. Bahr, P. Boudjouk, J.Org. Chem. 57 (1992) 5545.
[24] (a) M.D. Butts, G.J. Kubas, B.L. Scott, J. Am. Chem. Soc. 118 (1996) 11831. (b) B.A. Arndtsen, R.G. Bergman, Science 270 (1995) 1970.
[25] D. Huang, J.C. Huffman, J.C. Bollinger, O. Eisenstein, K.G. Caulton, J. Am. Chem. Soc. 119 (1997) 7398.
[26] T.D. Newbound, M.R. Colsman, M.M. Miller, G.P. Wulfsberg, O.P. Anderson, S.H. Strauss, J. Am. Chem. Soc. 111 (1989) 3762.
[27] M. Brown, J.M. Waters, J. Am. Chem. Soc. 112 (1990) 2442.
[28] G.R. Desiraju, Acc. Chem. Res. 24 (1991) 290.
[29] R. Taylor, O. Kennard, J. Am. Chem. Soc. 104 (1982) 5063.
[30] D. Braga, F. Grepioni, K. Biradha, V.R. Pedireddi, G.R. Desiraju, J. Am. Chem. Soc. 117 (1995) 3156.
[31] G.J. Kubas, J.E. Nelson, J.C. Bryan, J. Eckert, L. Wisnieski, K. Zilm, Inorg. Chem. 33 (1994) 2954.
[32] P.A. Maltby, M. Schlaf, M. Steinbeck, A.J. Lough, R.H. Morris, W.T. Klooster, T.F. Koetzle, R.C. Srivastava, J. Am. Chem. Soc. 118 (1996) 5396.
[33] T.A. Luther, D.M. Heinekey, Inorg. Chem. 37 (1998) 127.
[34] X.L. Luo, G.J. Kubas, J.C. Bryan, C.J. Burns, C.J. Unkefer, J. Am. Chem. Soc. 116 (1994) 10312.
[35] R.J. Ruszczyk, B.L. Huang, J.D. Atwood, J. Organomet. Chem. 299 (1986) 205.
[36] (a) E. Scharrer, S. Chang, M. Brookhart, Organometallics 14 (1995) 5686. (b) S. Chang, E. Scharrer, M. Brookhart, J. Mol. Catal. A 130 (1998) 107.
[37] G. Albertin, S. Antoniutti, S. Garcia-Fontan, R. Carballo, F. Padoan, J. Chem. Soc. Dalton Trans. (1998) 2071.
[38] B.T. Gregg, A.R. Cutler, Organometallics 13 (1994) 1039.
[39] SMART version 4.210, 1996, Bruker Analytical X-ray Systems Inc., 6300 Enterprise Lane, Madison, WI 53719.
[40] SAINT version 4.05, 1996, Bruker Analytical X-ray Systems Inc., Madison, WI 53719.
[41] SADABS, first release, George Sheldrick, University of Göttingen, Germany.
[42] $R_1 = \sigma||F_o| - |F_c||/\sigma|F_o|$ and $R_{2w} = [\Sigma[w(F_o^2 - F_c^2)^2]/\Sigma[w(F_o^2)^2]]^{1/2}$; $w = 1/[\sigma^2(F_o^2) + (0.0968*P)^2]$
[43] SHELXTL NT version 5.10, 1997, Bruker Analytical X-ray Instruments Inc., Madison, WI 53719.